Chemosphere 209 (2018) 640–653

Contents lists available at ScienceDirect

Chemosphere

journal homepage: www.elsevier.com/locate/chemosphere

Physiological, ultrastructural and proteomic responses of tobacco seedlings exposed to silver nanoparticles and silver nitrate

Petra Peharec Štefanić [a], Petra Cvjetko [a], Renata Biba [a], Ana-Marija Domijan [b], Ilse Letofsky-Papst [c], Mirta Tkalec [a], Sandra Šikić [d], Mario Cindrić [e], Biljana Balen [a, *]

[a] Department of Biology, Faculty of Science, University of Zagreb, Horvatovac 102a, 10000 Zagreb, Croatia
[b] Department of Pharmaceutical Botany, Faculty of Pharmacy and Biochemistry, University of Zagreb, Ante Kovačića 1, 10000, Zagreb, Croatia
[c] Institute of Electron Microscopy and Nanoanalysis (FELMI), Graz University of Technology, Graz Centre for Electron Microscopy (ZFE), Austrian Cooperative Research (ACR), Steyrergasse 17, 8010, Graz, Austria
[d] Department of Ecology, Andrija Štampar Teaching Institute of Public Health, Mirogojska cesta 16, 10000, Zagreb, Croatia
[e] Ruđer Bošković Institute, POB 1016, 10 000, Zagreb, Croatia

HIGHLIGHTS

- Higher accumulation of Ag was recorded after exposure to AgNPs compared to $AgNO_3$.
- Direct AgNPs uptake by root cells was confirmed.
- AgNPs induced less severe oxidative damage than $AgNO_3$.
- Ultrastructural and proteome study showed that AgNPs and $AgNO_3$ affect photosynthesis.
- Primary metabolism proteins were up-regulated after both types of treatments.

GRAPHICAL ABSTRACT

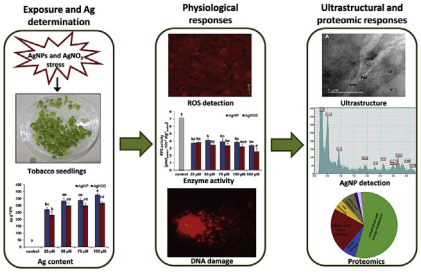

ARTICLE INFO

Article history:
Received 27 March 2018
Received in revised form
14 June 2018
Accepted 19 June 2018
Available online 20 June 2018

Handling Editor: Tamara S. Galloway

Keywords:
Silver nanoparticles
Nicotiana tabacum
Phytotoxicity
Ultrastructure
Proteomics

ABSTRACT

Since silver nanoparticles (AgNPs) are a dominant nanomaterial in consumer products, there is growing concern about their impact on the environment. Although numerous studies on the effects of AgNPs on living organisms have been conducted, the interaction of AgNPs with plants has not been fully clarified. To reveal the plant mechanisms activated after exposure to AgNPs and to differentiate between effects specific to nanoparticles and ionic silver, we investigated the physiological, ultrastructural and proteomic changes in seedlings of tobacco (*Nicotiana tabacum*) exposed to commercial AgNPs and ionic silver ($AgNO_3$) from the seed stage. A higher Ag content was measured in seedlings exposed to AgNPs than in those exposed to the same concentration of $AgNO_3$. However, the results on oxidative stress parameters obtained revealed that, in general, higher toxicity was recorded in $AgNO_3$-treated seedlings than in those exposed to nanosilver. Ultrastructural analysis of root cells confirmed the presence of silver in the form of nanoparticles, which may explain the lower toxicity of AgNPs. However, the ultrastructural changes of chloroplasts as well as proteomic study showed that both AgNPs and $AgNO_3$ can affect photosynthesis. Moreover, the majority of the proteins involved in the primary metabolism were up-regulated after both

* Corresponding author. Department of Biology, Faculty of Science, University of Zagreb, Horvatovac 102a, HR-10000, Zagreb, Croatia.
E-mail address: bbalen@biol.pmf.hr (B. Balen).

https://doi.org/10.1016/j.chemosphere.2018.06.128

types of treatments, indicating that enhanced energy production, which can be used to reinforce defensive mechanisms, enables plants to cope with silver-induced toxicity.

1. Introduction

Compared to the parent bulk materials, nanoparticles (NPs) with three dimensions between 1 and 100 nm, have unique and advanced electrical, chemical and physical properties. The large surface area to volume ratio increases their biological activity. These properties bring to the nanotechnology products a significant market potential, but also underline a whole range of uncertainties regarding the impact on the environment and human health (Maynard et al., 2011; Beer et al., 2012). Silver nanoparticles (AgNPs) are of particular interest because of their well-known antibacterial and antifungal properties that are successfully exploited in medical applications and devices, textiles, food packaging, and healthcare and household products (Kim et al., 2009; Ahamed et al., 2010; Zhang et al., 2016). AgNPs are the most commonly used nanomaterial in consumer products (Calderón-Jiménez et al., 2017), so it can be expected that these particles will be abundantly released into the environment, in which they may affect different types of organisms. Studies on AgNP toxicity showed mostly deleterious effects on bacteria, animals, human cells, algae and plants (Navarro et al., 2008a; Tripathi et al., 2017). However, the mechanisms of AgNP toxicity have not been fully elucidated; they may be related to the nanoparticle-specific effects (Powers et al., 2011; Poynton et al., 2012), but also to the effects of ionic silver released from AgNPs (Navarro et al., 2008b; Piccapietra et al., 2012). Numerous *in vitro* and *in vivo* tests provide information that the toxic behaviour of AgNPs towards a variety of organisms might be caused by the disruption of cell membrane integrity (Castiglioni et al., 2014; Zhang et al., 2014), the formation of reactive oxygen species (ROS) (Abdal Dayem et al., 2017; Cvjetko et al., 2017), and oxidative damage to biologically important macromolecules such as proteins and DNA (Mytych et al., 2017; Cvjetko et al., 2017).

Toxicological studies of AgNPs conducted on plants, primary producers necessary for the functioning of the ecosystem, indicate that the effects that AgNPs can induce in higher plants depend on the plant species and age, the nanoparticle size and concentration, as well as on the test conditions i. e. temperature, duration and method of exposure (El-Temsah and Joner, 2012; Lee et al., 2012; Sharma et al., 2012; Yin et al., 2012). It has been shown that AgNPs can enter plant cells directly, mostly through the cell wall of the root cells (Tripathi et al., 2017), the vacuoles of which seem to be the primary storage for AgNP accumulation (Vannini et al., 2014; Yin et al., 2011; Cvjetko et al., 2018). As a response to stress imposed by AgNPs many authors reported an increase in ROS formation, accompanied by the enhanced activities of antioxidant enzymes (Jiang et al., 2014; Tripathi et al., 2017; Cvjetko et al., 2017, 2018). Moreover, AgNPs were also found to induce DNA damage (Cvjetko et al., 2017, 2018) and influence gene expression (Patlolla et al., 2012; Qian et al., 2013; Saha and Dutta Gupta, 2017).

As the model organism in this research we used tobacco, an economically interesting plant that is frequently used as a model species in abiotic stress research (Peharec Štefanić et al., 2012; Tkalec et al., 2014; Majsec et al., 2016). Tobacco is an extremely versatile system for all aspects of cell and tissue culture research (Ganapathi et al., 2004) and relatively tolerant to environmental stress (Schaeffer et al., 2012). Moreover, since the tobacco genome sequence has been published (Sierro et al., 2014), it is also a convenient species on which to study changes at the proteome level. In a prior study, we investigated the phytotoxicity of citrate-coated AgNPs on fully developed adult plants of tobacco (*Nicotiana tabacum* L.), in which after 7-day exposures, AgNPs were found to be less toxic than ionic silver (Cvjetko et al., 2018). AgNP treatments did not induce significant oxidative stress either in roots or in leaves, even though AgNP uptake in root cells was proven. In this study, our aim was to investigate whether the phytotoxic effects of AgNPs could be observed in tobacco seedlings, at a more vulnerable stage of growth, which were exposed to AgNPs from the seed stage, and whether AgNP toxicity could be attributed to nanoparticles or to ionic silver. Furthermore, to examine the molecular bases of AgNP phytotoxicity, we also analyzed the proteome of seedlings. Namely, changes in protein expression and identification of protein markers have been proven to be a powerful approach to the identification of proteins related to specific developmental and/or environmental signals (Gygi and Aebersold, 2000). Although proteomic approaches have contributed extensively to an increase of the knowledge of the molecular mechanisms of plant response to heavy metals (Hossain and Komatsu, 2013; Cvjetko et al., 2014), only a few studies dealing with proteome changes have been carried out to analyse the effects of AgNPs in plant cells (Vannini et al., 2013, 2014; Mustafa et al., 2015).

2. Materials and methods

2.1. AgNPs and $AgNO_3$ suspensions

All experiments were performed with commercial citrate-coated AgNPs (50 nm Citrate NanoXactTM Silver, Nanocomposix, San Diego, CA, ζ potential of −47.8 mV). The concentration of AgNP stock solution was 0.021 mg mL^{-1}. Silver nitrate ($AgNO_3$, Sigma-Aldrich) was dissolved in ultrapure Milli-Q water and used as a 100 mM stock solution. For preparation of AgNP solutions the concentration of Ag was taken into account in calculations. Prior to treatments, Ag concentration in AgNP solutions was determined by ELAN DRC-e ICP-MS (Perkin Elmer, USA) as described in section 2.4, which confirmed the required Ag concentration.

2.2. Plant material and culture treatments

The exposure experiment was conducted in plant tissue culture conditions using solid Murashige and Skoog (MS) nutrient medium (0.9% Phytagel agar, 3% sucrose) (Murashige and Skoog, 1962) in Petri dishes (90 mm diameter). After sterilization, the medium was supplemented with AgNPs or $AgNO_3$ (as ionic silver) stock solution to obtain the following concentrations: 25, 50, 75 and 100 μM. Tobacco (*Nicotiana tabacum* L.) cv. Burley seeds were sterilized with 50% (v/v) NaOCl for 15 min, rinsed 6 × with deH_2O and subsequently planted on the MS nutrient medium (50 seeds per Petri dish). Control material was cultivated by placing the seeds on MS medium that was devoid of either AgNPs or $AgNO_3$. The experiment was conducted in the culture room at 24 ± 1 °C with 16/8 h light/dark cycles and a light intensity of 90 μmol m^{-2} s^{-1}. Under these conditions seeds started to germinate after 2–3 days and grew into fully developed seedlings with 3–4 true leaves within 30 days.

Eventually the exposure period lasted for 30 days, after which whole seedlings were harvested and used for analyses. All exposure treatments were conducted three times. In each experiment, there were three replicates of every AgNP or $AgNO_3$ concentration (three Petri dishes per concentration).

2.3. AgNP stability in culture medium

MS medium with dissolved Phytagel agar was supplemented with AgNP stock solution to obtain a 100 μM concentration (resulting in phytotoxic effects in treatments with nanoparticles) just prior to solidification; then it was quickly poured in Petri dish and left to solidify. In parallel, a 1 mL aliquot of this solution was quickly pipetted to the 1-cm quartz cuvette and left to solidify completely (within a few minutes) for spectrophotometric absorbance measurements. Petri dish and cuvette with solid MS medium were sealed with Parafilm M to prevent media drying and kept in the same conditions as plant material during three weeks. To check stability of AgNPs in solid MS medium, a piece (1 × 1 cm) of medium was cut out from the Petri dish after three weeks, placed between two microscopic slides and analyzed using dark-field microscopy. Spectrophotometric absorbance measurements were performed using the UV–visible spectrophotometer in the wavelength range of 300–800 nm. For instrument zeroing, solidified MS medium devoid of AgNPs was used. Stability of AgNPs was monitored regularly during three weeks.

2.4. Determination of Ag content

Whole seedlings were washed with 0.01 M HNO_3, rinsed with ultrapure Milli-Q water and dried to constant weight at 80 °C (approximately 24 h). Dried tissue samples (0.1 g) were prepared as previously reported (Cvjetko et al., 2017, 2018). Determination of the total Ag concentration was performed using an ELAN DRC-e ICP-MS (Perkin Elmer, USA). To calculate the Ag concentration we used a calibration curve obtained with a set of standards of known concentrations. Detection limit and limit of quantification (LOQ) were 0.05 mg kg^{-1} and 0.1 mg kg^{-1} respectively. Spike recovery tests were 96.6% and 96.8% for seedlings exposed to AgNPs and $AgNO_3$, respectively.

2.5. Determination of oxidative stress parameters

Dihydroethidium (DHE) test was used to determine the ROS level as previously described (Cvjetko et al., 2017, 2018). After washing, plant material was transferred to microscopic slides, which were examined under an Olympus BX-51 fluorescent microscope at excitation wavelength 450–490 nm and emission wavelength 520 nm or more. In 10 fields of each slide, the total number of at least 100 randomly chosen cells was analyzed for fluorescence intensity with computer software Lucida 6.0 (Wirral, UK). Results are expressed as relative fluorescence intensity compared to control seedlings.

Lipid peroxidation was determined by measuring the malondialdehyde (MDA) content according to a modified Heath and Packer (1968) method as published in Cvjetko et al. (2018). The content of MDA was expressed as μmol g^{-1} of fresh weight ($\varepsilon = 155\ mM^{-1}\ cm^{-1}$).

Extraction of total soluble proteins was performed according to Cvjetko et al. (2018). Protein content was determined according to Bradford (1976). These supernatants were used for protein carbonyl quantification and enzyme assays.

For protein carbonyl quantification the method of Levine et al. (1990) was applied. Samples were prepared as previously reported (Cvjetko et al., 2018). Carbonyl content was expressed as μmol mg^{-1} of proteins.

For the assessment of genotoxicity, we applied an alkaline version of the Comet assay (Gichner et al., 2004) under slightly modified conditions (Cvjetko et al., 2017, 2018) to measure the percentage of tail DNA (% tDNA).

Superoxide dismutase (SOD, E.C. 1.15.1.1) activity was determined by NBT photo reduction (Beauchamp and Fridovich, 1971). The reaction mixture composition and measurement parameters are described in detail in Cvjetko et al. (2018). Activity was expressed as units of SOD activity mg^{-1} of protein.

For peroxidase (PPX, E.C. 1.11.1.7) and ascorbate peroxidase (APX, E.C. 1.11.1.11) activity measurements we used the original method of Nakano and Asada (1981) with slight modifications (Cvjetko et al., 2017, 2018). The activities were expressed as μmol of purpurogallin min^{-1} mg^{-1} of protein ($\varepsilon = 2.6\ mM^{-1}\ cm^{-1}$) for PPX and as μmol of ascorbate min^{-1} mg^{-1} of protein ($\varepsilon = 2.8\ mM^{-1}\ cm^{-1}$) for APX.

Catalase (CAT, E.C. 1.11.1.6) activity was measured according to the protocol of Aebi (1984) and Cvjetko et al. (2017; 2018). It was expressed as μmol of H_2O_2 min^{-1} mg^{-1} of protein ($\varepsilon = 36\ mM^{-1}\ cm^{-1}$).

2.6. Microscopy analyses and determination of photosynthetic pigments

Tobacco seedlings treated with 100 μM AgNP and 100 μM $AgNO_3$ were used to study morphological and ultrastructural changes and to detect the uptake of nanoparticles in plant cells. Small pieces of leaflets and 3 mm long roots were fixed and post-fixed in 0.5 M cacodylate buffer (pH 7.2). The specimens were washed in the same buffer, dehydrated in ethanol (50%–100%) and embedded in Spurr's resin as described previously (Cvjetko et al., 2018). Semithin and ultrathin sections were prepared with an ultramicrotome Leica Ultracut R (Leica, Germany) and stained. An Olympus BX-51 microscope was used for structural analyses, while FEI Morgagni 268D and monochromated TF20 (FEI Tecnai G2) electron microscopes were used for ultrastructural study and for confirmation of the localization of AgNPs in the tobacco cells, respectively.

Leaves (0.10 g) from seedlings treated with 100 μM AgNP and 100 μM $AgNO_3$ were homogenized in 2 mL of 100% acetone and homogenates were centrifuged for 10 min at 5000 g and 4 °C. Chlorophyll *a*, chlorophyll *b* and carotenoid contents were determined by measuring the absorbance of supernatants at 645, 663 and 470 nm and calculated according to Lichtenthaler (1987) and Wellburn (1994).

2.7. Statistical analysis

To compare the results, we used analysis of variance (ANOVA) followed by Newman-Keuls post-hoc test (STATISTICA 10.0, Stat Soft Inc., USA). Differences between means were considered statistically significant at $P \leq 0.05$. Each data point is the average of nine replicates from three experiments, unless stated otherwise.

2.8. Proteomic analyses

Changes in protein expression were analyzed in seedlings treated with 100 μM AgNPs and 100 μM $AgNO_3$. Whole seedlings (1.5 g) were used to isolate proteins by phenol extraction (Faurobert et al., 2007; Pavoković et al., 2012). Two-dimensional (2-DE) electrophoresis was conducted to separate proteins (Rogić et al., 2015). ImageMaster 2D Platinum software version 7.0 (GE Healthcare, USA) was used for protein detection and image analysis. Protein spots that exhibited a ±1.5-fold change and $P \leq 0.05$ were considered as differentially expressed.

Protein spots were excised from the gels and subjected to trypsin digestion as previously described (Rogić et al., 2015). Peptides were dissolved in 0.1% (v/v) TFA (Shevchenko et al., 1996), purified using Bravo Automated Liquid Handling Platform on RP-S cartridges (AssayMAP Bravo, Agilent Technologies, USA) and dried.

Peptides obtained were dissolved in 4 μL of 5 mg mL^{-1} a-cyano-4-hydroxycinnamic acid matrix prepared in 50% TFA ($\varphi = 0.1\%$) in acetonitrile, and analyzed with a matrix-assisted laser desorption/ionization–time-of-flight mass spectrometer (4800 Plus MALDI TOF/TOF analyzer, Applied Biosystems, USA), working in positive reflector mode. In MS analysis, 1600 shots were taken per spectrum, while 2000 shots were acquired in MS/MS analysis, covering the mass range of 900–4000 Da, focus mass 2000 Da and delay time 450 ns The spectra analyses were performed using parameters previously reported (Rogić et al., 2015).

The global protein server explorer software (version 3.6, Applied Biosystems, USA) for Mascot (Matrix Science version 2.1, UK) search against National Center for Biotechnology Information protein database (NCBIprot, http://www.ncbi.nlm.nih.gov/protein) was applied for protein identification. Monoisotopic peptide masses were used for combined MS and MS/MS database searches with the following search parameters: MS/MS mass fragment tolerance 0.5 Da, mass precursor tolerance 0.3 Da, a maximum of one incomplete cleavage per peptide, peptide charge +1. All searches were evaluated based on the significant scores obtained from Mascot. Identified proteins are presented in Table S1. Only the spots with a fold change of ±1.5 and ANOVA $P \leq 0.05$ were accepted as differentially expressed. Universal Protein Resource (UniProt) was used for Gene ontology (GO, http://www.geneontology.org) analysis for all identified proteins.

3. Results

3.1. AgNPs stability in culture medium

The results of the AgNP (100 μM concentration) stability analyses in solid MS medium are presented in Fig S1. Spectrophotometric absorbance measurements showed reduction of the absorption maximum immediately after solidification of the medium (zero minute) and a peak shift towards lower wavelengths (peak maximum at 414 nm) compared to the absorption maximum obtained for the 100 μM AgNP solution in Milli-Q water (peak maximum at 424 nm) (Fig. S1A). Afterwards, the absorption maximum and peak position remained mostly stable during the period of three weeks with a minor decrease in the absorption maximum and a slight shift of a peak towards lower wavelengths. Additionally, dark-field microscopy verified uniform distribution of AgNPs in solid medium after three weeks (Fig. S1B).

3.2. Ag content and phytotoxic effects

Significant Ag uptake was measured in seedlings after exposure to either AgNPs or $AgNO_3$ compared to the control (Table 1). The content of Ag was higher after the exposure to AgNPs than to $AgNO_3$. This was particularly pronounced after the exposure to 100 μM AgNPs, where a significantly higher value was obtained than in the corresponding treatment with $AgNO_3$ (Table 1). In control seedlings, Ag content was below the instrument LOQ (<0.1 μg g^{-1}).

To determine the potential phytotoxic effect of AgNPs and $AgNO_3$ in tobacco seedlings, oxidative stress parameters were measured after exposure to increasing concentrations of both silver forms. Results are presented in Table 1. Treatments with $AgNO_3$ induced significant oxidative stress in tobacco seedlings; higher ROS formation was observed from the 50 μM concentration and resulted in elevated MDA and carbonyl contents compared to the control. Furthermore, comet assay revealed that $AgNO_3$ induced an increase in tail DNA from even the lowest (25 μM) concentration applied. In contrast, exposure to AgNP-treatments resulted in significantly increased values of oxidative stress parameters only after the highest (100 μM) applied concentration of AgNPs.

Beside oxidative stress parameters, changes in activities of antioxidant enzymes were also determined (Table 2). All applied AgNP-treatments significantly elevated SOD activity, especially exposure to the highest tested concentration (100 μM). Among the $AgNO_3$ treatments, only two lower concentrations (25 and 50 μM) significantly induced SOD activity compared to the control. Furthermore, exposure to all applied AgNP and $AgNO_3$ treatments significantly elevated APX activity, with the exception of the treatment with 25 μM $AgNO_3$. In contrast, exposure to all AgNP and $AgNO_3$ concentrations induced a significant reduction in PPX activity compared to the control seedlings. CAT activity did not change after exposure to AgNPs, while $AgNO_3$ treatments induced reduction in CAT activity, which was significant after the exposure to 75 and 100 μM $AgNO_3$.

3.3. Morphological and ultrastructural changes and AgNP localization

Seedlings treated with 100 μM AgNP and 100 μM $AgNO_3$ exhibited significantly reduced roots (Figs. S2A and B) and chlorotic leaves (Fig. S2C) compared to the control. However, light microscopy did not reveal any significant changes in the organization of root apical meristem and elongation zone in the AgNP-treated seedlings compared to the control (Fig. 1A and B). In contrast, the roots of the $AgNO_3$-treated seedlings were thicker with a reduced root cap (Fig. 1C). On the ultrastructural level neither AgNPs nor

Table 1
Contents of silver, reactive oxygen species (ROS), malondialdehyde (MDA), protein carbonyl and % tail DNA in tobacco seedlings after 30 days of exposure to 0, 25, 50, 75 and 100 μM AgNPs and $AgNO_3$.

	Conc. (μM)	Ag (μg g^{-1} DW)	ROS (% of control)	MDA (μmol g^{-1} FW)	Protein carbonyl (μmol mg^{-1} protein)	% tail DNA
Control	0	0[a,a]	100 ± 1.15^{a}	6.00 ± 0.34^{a}	0.054 ± 0.006^{a}	7.14 ± 0.48^{a}
AgNP	25	271.27 ± 14.71^{bc}	109.59 ± 7.46^{a}	6.14 ± 0.34^{a}	0.057 ± 0.009^{abc}	7.82 ± 0.70^{ab}
	50	333.31 ± 22.60^{de}	108.85 ± 7.11^{a}	6.99 ± 0.26^{ab}	0.059 ± 0.009^{abc}	8.34 ± 0.69^{ab}
	75	336.18 ± 18.59^{de}	108.34 ± 7.83^{a}	6.85 ± 0.73^{ab}	0.055 ± 0.008^{ab}	8.18 ± 0.78^{ab}
	100	375.63 ± 9.96^{e}	128.28 ± 7.61^{bc}	7.79 ± 0.56^{bc}	0.067 ± 0.007^{cd}	11.60 ± 0.86^{cd}
$AgNO_3$	25	230.39 ± 28.10^{b}	111.82 ± 8.22^{ab}	7.92 ± 0.28^{bc}	0.062 ± 0.008^{bc}	10.14 ± 0.77^{bc}
	50	298.36 ± 18.33^{cd}	128.02 ± 7.57^{bc}	8.66 ± 0.35^{c}	0.070 ± 0.009^{d}	12.38 ± 0.95^{cd}
	75	299.20 ± 14.17^{cd}	127.71 ± 9.83^{bc}	11.11 ± 0.08^{d}	0.068 ± 0.009^{d}	14.17 ± 0.99^{e}
	100	316.51 ± 11.51^{cd}	131.55 ± 8.89^{c}	10.18 ± 0.18^{d}	0.067 ± 0.008^{cd}	12.94 ± 0.91^{de}

Values are the means ± SE of three different experiments, each with three replicas. If values are marked with different letters, the treatments are significantly different at $P \leq 0.05$ according to Duncan test.
[a] Silver content was below the limit of quantification (<0.1 μg g^{-1}).

Table 2
Differences in specific activities of superoxide dismutase (SOD), pyrogallol peroxidase (PPX), ascorbate peroxidase (APX) and catalase (CAT) in tobacco seedlings after 30 days of exposure to 0, 25, 50, 75 and 100 μM AgNPs and $AgNO_3$.

	Conc. (μM)	SOD activity (U mg^{-1} protein)	PPX activity (μmol product min^{-1} mg^{-1} protein)	APX activity (μmol product min^{-1} mg^{-1} protein)	CAT activity (μmol H_2O_2 min^{-1} mg^{-1} protein)
Control	0	1.93 ± 0.14^{a}	7.17 ± 1.03^{a}	0.063 ± 0.002^{a}	0.178 ± 0.01^{bc}
AgNP	25	3.23 ± 0.64^{bc}	3.72 ± 0.64^{b}	0.104 ± 0.009^{b}	0.217 ± 0.03^{c}
	50	3.420 ± 0.62^{c}	4.11 ± 0.65^{b}	0.109 ± 0.009^{b}	0.163 ± 0.02^{bc}
	75	3.23 ± 0.69^{bc}	3.93 ± 0.64^{b}	0.115 ± 0.009^{b}	0.159 ± 0.03^{abc}
	100	5.39 ± 0.65^{d}	3.83 ± 0.35^{b}	0.128 ± 0.00^{bc}	0.172 ± 0.02^{bc}
$AgNO_3$	25	5.64 ± 0.86^{d}	3.81 ± 0.91^{b}	0.070 ± 0.008^{a}	0.148 ± 0.02^{ab}
	50	2.99 ± 0.55^{bc}	3.43 ± 0.65^{b}	0.107 ± 0.006^{b}	0.125 ± 0.03^{ab}
	75	2.38 ± 0.34^{a}	3.37 ± 0.97^{b}	0.119 ± 0.008^{bc}	0.102 ± 0.02^{a}
	100	2.74 ± 0.27^{abc}	3.21 ± 0.47^{b}	0.144 ± 0.009^{c}	0.100 ± 0.02^{a}

Values are the means ± SE of three different experiments, each with three replicas. If values are marked with different letters, the means are significantly different ($p \leq 0.05$) according to Duncan test.

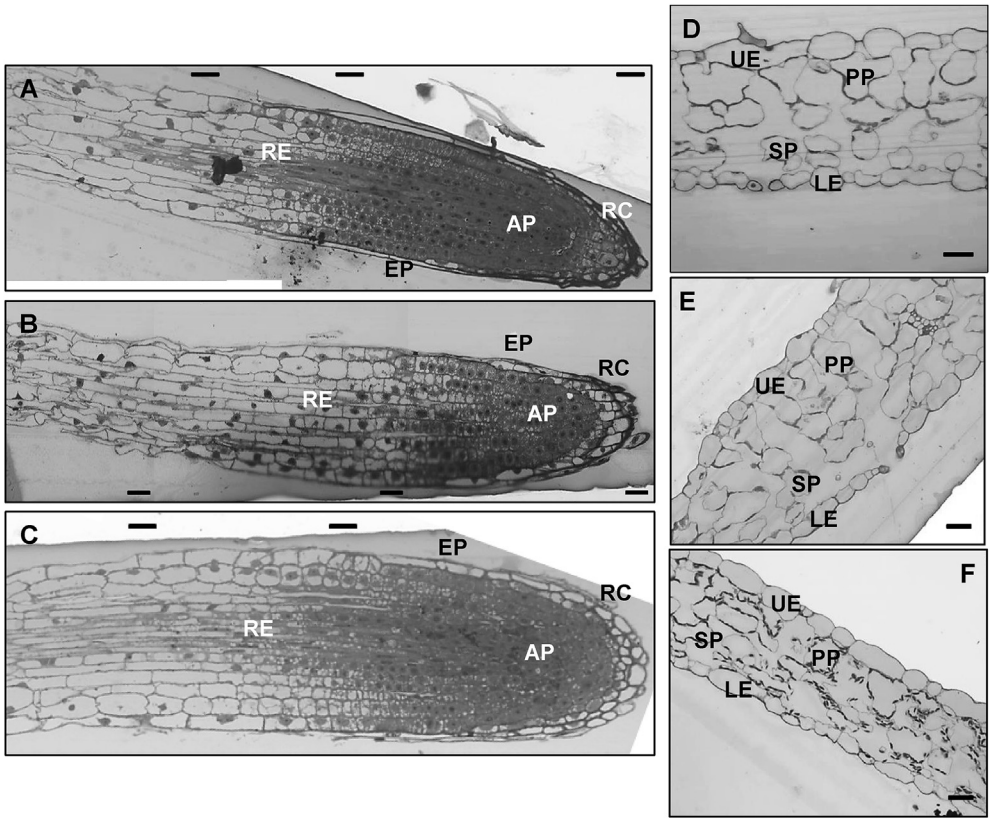

Fig. 1. Semithin sections of root from (A) control, (B) 100 μM AgNP-treated and (C) 100 μM $AgNO_3$-treated tobacco seedlings (bar = 33.1 μm) and leaf from (D) control, (E) 100 μM AgNP-treated and (F) 100 μM $AgNO_3$-treated tobacco seedlings (bar = 30.6 μm). RC – root cap, AP – apical meristem, RE – region of elongation, EP – epidermis, UE – upper epidermis, LE – lower epidermis, PP – palisade parenchyma, SP – spongy parenchyma.

$AgNO_3$ induced changes in the root cells organization (Fig. 2A–C), but in AgNP-exposed seedlings particles were visible in the intercellular space (Fig. 3A and B). The energy-dispersive X-ray (EDX) scan confirmed that the particles contained silver (Fig. 3C), which proves that the AgNPs have been directly uptaken by root cells, in which they accumulated.

Leaf semithin sections showed no significant changes in the cell organization in AgNP-treated seedlings compared to the control (Fig. 1D and E), while leaves of $AgNO_3$-treated seedlings were thinner with bigger chloroplasts in the cells (Fig. 1F). Ultrastructural studies revealed changes in chloroplasts in the leaves of both AgNP– and $AgNO_3$-treated seedlings (Fig. 2D–F). The chloroplasts of seedlings exposed to AgNPs were swollen with dilated thylakoid systems and bigger plastoglobules than the control (Fig. 2E). Chloroplasts of the $AgNO_3$-treated seedlings were round in shape, swollen with no thylakoid system formation, ruptured and contained bigger plastoglobules (Fig. 2F). In the leaf tissue, AgNPs could not be detected.

To confirm the impact of AgNPs and $AgNO_3$ on chloroplast, photosynthetic pigments were also measured. The content of chlorophyll *a and b* and the content of carotenoids were significantly reduced in both treatments (Fig. S2D). Moreover, the decrease was more pronounced after exposure to $AgNO_3$ than to AgNPs.

3.4. Proteome changes

Representative gels presenting proteomes of the control

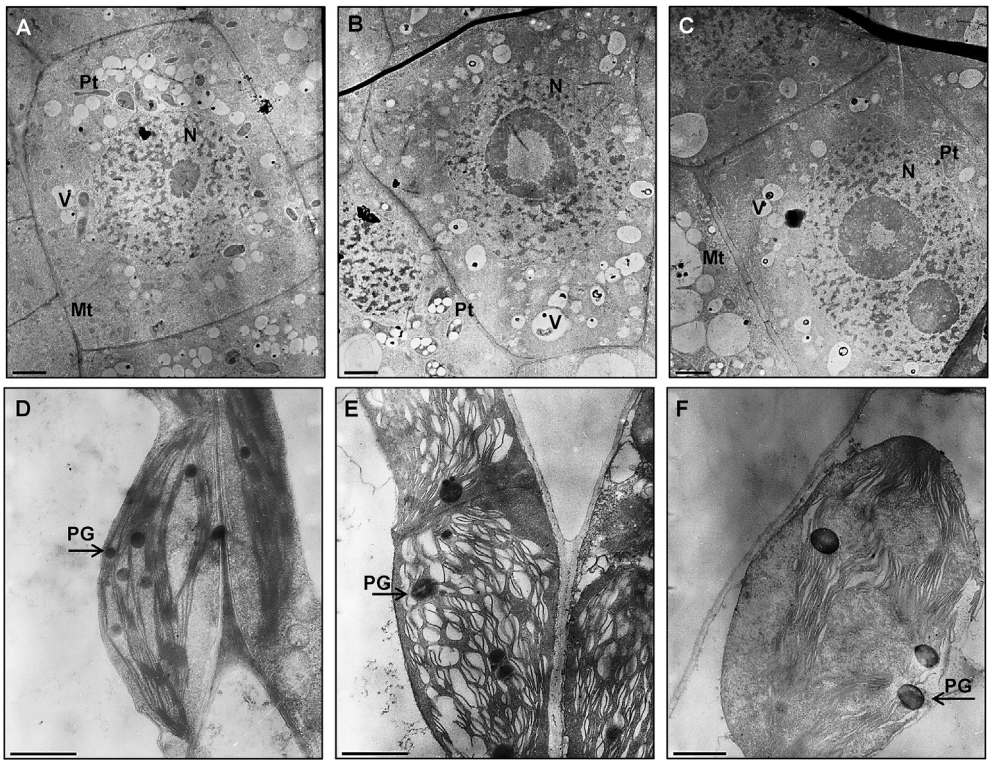

Fig. 2. Ultrastructure of root cells and leaf chloroplasts. Root cells of (A) control, (B) 100 μM AgNP-treated and (C) 100 μM $AgNO_3$-treated tobacco seedlings (bars = 2 μm). Chloroplasts in leaf cells of (D) control, (E) 100 μM AgNP-treated and (F) 100 μM $AgNO_3$-treated tobacco seedlings (bars = 1 μm). N – nucleus, V – vacuole, Mt – mitochondrion, Pt – plastid, PG – plastoglobules.

seedlings and seedlings treated with 100 μM AgNPs and $AgNO_3$ are shown in Fig. S3. Out of more than 500 detected protein spots, 69 spots revealed significantly different expression between control and seedlings exposed to either AgNPs or $AgNO_3$. Among these, 58 were found to be responsive to AgNP-treatment (Fig. S3B; Table S1), while 67 showed different expressions after exposure to $AgNO_3$ (Fig. S3C; Table S1). Among AgNP-responsive proteins, 55 were up-regulated and 3 were down-regulated, while after exposure to $AgNO_3$, 66 proteins were found to be up-regulated and one down-regulated compared to control (Table S1).

An overlap of 57 proteins was observed between proteins differentially expressed in response to both AgNPs and $AgNO_3$, among which 56 proteins were up-regulated in both treatments; one was down-regulated in response to AgNPs but up-regulated in response to $AgNO_3$. Ten proteins were responsive only to the presence of $AgNO_3$, among which 9 proteins were up-regulated. Two proteins responded only to the AgNPs and were down-regulated (Table 3).

Out of 69 differentially expressed proteins revealed after either AgNP– or $AgNO_3$– treatment, 67 were identified in the Viridiplantae subset of the NCBInr. For a broader classification, identified proteins were subjected to gene ontology (GO) analysis in the Uniprot database, after which proteins were classified into eight functional categories according to their putative biological process (Fig. 4; Table 3). The majority of the proteins belonged to the "carbohydrate and energy metabolism" group (54.24% and 50.75% after AgNP– and $AgNO_3$-treatments, respectively), although category "defense and stress response" was also highly represented (22.03% and 23.88% after exposure to AgNPs and $AgNO_3$, respectively). The category "protein synthesis" was represented with 6.78% of proteins after AgNP-treatment and 8.96% after treatment with $AgNO_3$. The percentage of 5.08 and 4.48 of total proteins was calculated for the "RNA processing" category after exposure to AgNPs and $AgNO_3$ respectively, while proteins belonging to the category of "amino acid metabolism" were represented with 6.78% after AgNP-treatment and 5.97% after treatment with $AgNO_3$. Proteins from the "nucleotide metabolism" and "cell signal cascades" categories were represented with 1.69% and 1.49% after exposure to AgNPs and $AgNO_3$ respectively. 2.44% (AgNP-exposure) and 3.17% ($AgNO_3$-exposure) of the proteins were assigned to the "unknown" functional category.

Identified proteins that were up-regulated by both AgNP– and $AgNO_3$-treatments were found in all functional categories. The only protein that was down-regulated by $AgNO_3$-treatment, PsaE, is involved in "carbohydrate and energy metabolism" (Table 3). Two out of three proteins down-regulated by AgNP-treatment belong to "carbohydrate and energy metabolism", while protein beta chaperonin 60, which was also up-regulated by $AgNO_3$, is involved in the "defense and stress response". In total, 13 proteins had different expression depending on $AgNO_3$/AgNP treatment (Table 3).

4. Discussion

Toxicity of AgNPs in plant cells can be attributed to the generation of ROS (Mirzajani et al., 2013; Nair and Chung, 2014a), the increased production of which in cells is often connected with higher AgNP uptake (Tripathi et al., 2017; Cvjetko et al., 2017). Qian et al. (2013) and Nair and Chung (2014a) suggested that higher Ag accumulation in plants exposed to AgNPs might be a result of their direct uptake and/or AgNPs could get oxidized on the root surface and release Ag^+, which can enter the root tissue directly without dissolving in the solution. However, despite the higher accumulation of Ag in seedlings exposed to AgNPs than in those exposed to $AgNO_3$, AgNPs applied in concentrations lower than 100 μM did not

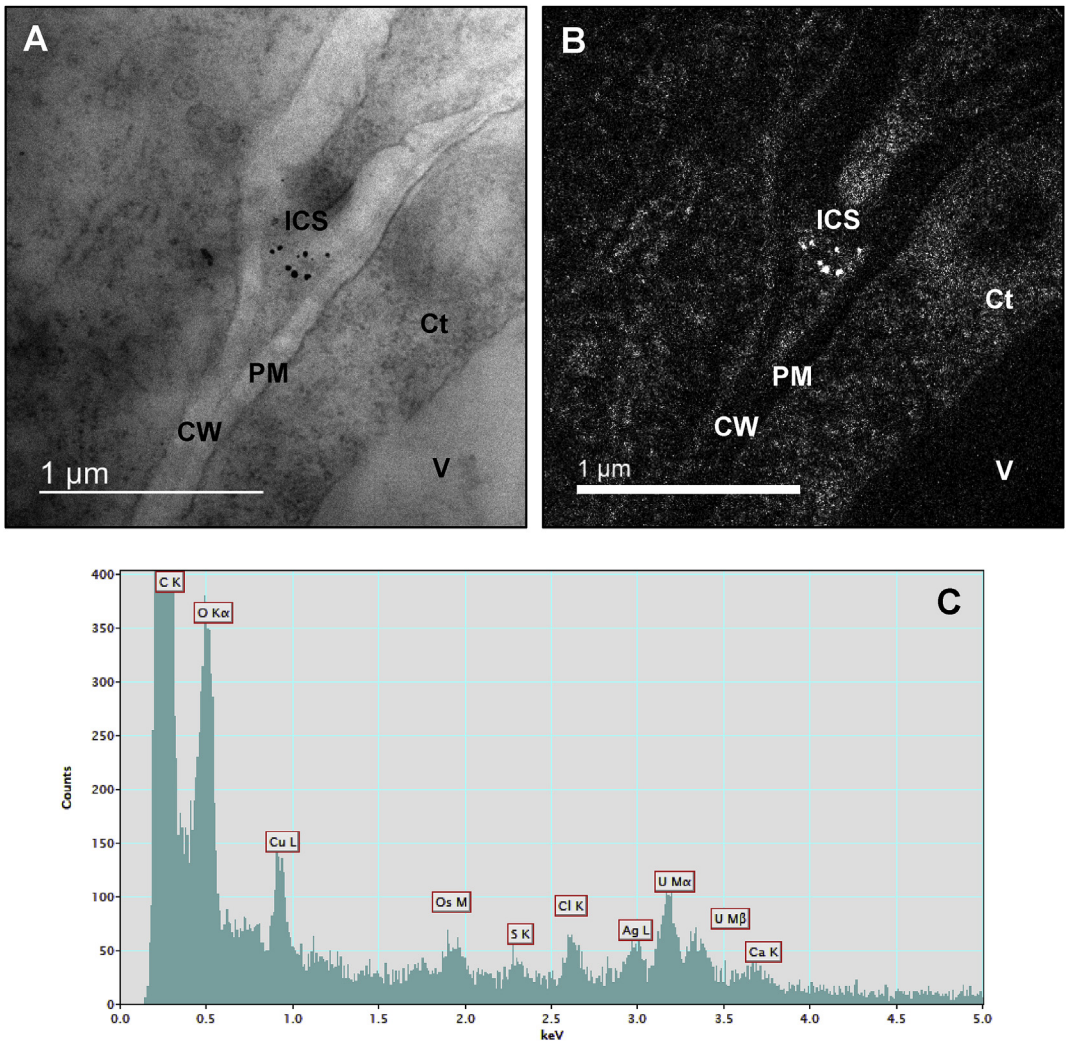

Fig. 3. AgNP localization in the root cells of the 100 µM AgNP-treated tobacco seedlings. TEM images of (A) silver nanoparticles, (B) bright field images, and (C) energy-dispersive X-ray spectrum. V – vacuole, CW – cell wall, PM – plasma membrane, Ct – cytoplasm, ICS – intercellular space.

increase ROS formation or cause oxidative stress, in contrast to the results obtained with $AgNO_3$. Similar findings were also obtained in adult tobacco plants (Cvjetko et al., 2018). Moreover, effects of $AgNO_3$ more toxic than those of AgNPs have already been reported for Arabidopsis seedlings (Nair and Chung, 2014b) and *A. cepa* roots (Cvjetko et al., 2017). Our results suggest the direct uptake of silver nanoparticles in root cells, as proven by EDX-TEM analysis, and imply that AgNPs remained mainly in the form of nanoparticles after entering the cells. Therefore, AgNPs caused less severe oxidative damage than the Ag^+ originating from an $AgNO_3$ salt. Moreover, enhanced SOD activity was found in the majority of AgNP-exposed tobacco seedlings, which is in agreement with the low level of oxidative damage. Neutralization of $O_2^{\cdot-}$ by SOD is very effective in preventing damage to biologically important molecules. The induction of SOD activity was additionally confirmed by proteomic analysis, where up-regulation of Fe-SOD was found. In several other plant species increased SOD activity and expression were also reported after AgNP-treatments (Vannini et al., 2013; Rani et al., 2016). As for the $AgNO_3$, in seedlings exposed to the lower concentrations (25 and 50 µM) SOD activity increased; however, higher $AgNO_3$ concentrations decreased it, thus resulting in observed oxidative damage. Reduced SOD activity at higher $AgNO_3$ concentrations may reflect the over-accumulation of ROS, which exceeded the scavenging ability of antioxidant defense systems (Hatami and Ghorbanpour, 2013; Cvjetko et al., 2018). It has been reported that Ag^+ ions can affect enzyme activities by binding to thiols and other active groups or by displacing native metal cations from their binding sites in enzymes (Ghandour et al., 1988). To protect cells against ROS completely, antioxidant enzymes such as CAT, PPX and APX have to remove H_2O_2 generated by SOD dismutation of $O_2^{\cdot-}$. In our study, elevated APX activity, along with the decreased PPX and either unchanged (AgNPs) or decreased ($AgNO_3$) CAT activity, suggests that APX is a key enzyme catalyzing the conversion of H_2O_2 into H_2O in tobacco seedlings exposed to either AgNPs or $AgNO_3$. Moreover, the proteomic study revealed three up-regulated proteins after exposure to both types of treatment, which were identified as APX. Elevated APX activity was also recorded in *Pelargonium zonale* leaves after treatment with AgNPs (Hatami and Ghorbanpour, 2013) and *Fragaria* x *ananassa* exposed to $AgNO_3$ (Qin et al., 2005), which corroborates our results. However, despite the enhanced activity of SOD and APX, increased parameters of oxidative stress were observed in seedlings treated with 100 µM AgNP. This was in correlation with the prominent reduction of root growth, chlorosis of leaves and the reduced content of chlorophylls and carotenoids, which was also found in these seedlings. Moreover, microscopy analysis revealed swollen

Table 3
List of differentially expressed proteins in tobacco seedlings treated with 100 μM AgNPs or 100 μM $AgNO_3$ with the respect to the control with assigned biological process. Proteins were identified by MALDI-TOF/TOF MS/MS and Mascot search against NCBIprot database.

Spot(s) No.[a]	Protein name	Biological process[b]	Differential expression[c]
Carbohydrate and energy metabolism			
7	Chloroplast ATP synthase CF1 beta subunit	ATP synthesis coupled proton transport	AgNP ↑, $AgNO_3$ ↑
8	Plastid ATP synthase CF1 beta subunit	ATP synthesis coupled proton transport	AgNP ↑, $AgNO_3$ ↑
9	Phosphoglycerate mutase, 2,3-bisphosphoglycerate-independent	Glycolytic process	AgNP =, $AgNO_3$ ↑
12, 13, 24, 27	Ribulose bisphosphate carboxylase/oxygenase activase 2	Activation of Rubisco	AgNP ↑, $AgNO_3$ ↑
20, 21	Glyceraldehyde-3-phosphate dehydrogenase	Glucose metabolic process	AgNP ↑, $AgNO_3$ ↑
22	Putative mitochondrial NAD-dependent malate dehydrogenase	Tricarboxylic acid cycle	AgNP ↑, $AgNO_3$ ↑
25	Chloroplast ferredoxin-NADP + oxidoreductase precursor	Photosynthesis	AgNP =, $AgNO_3$ ↑
28, 29	Plastidic aldolase	Glycolytic process	AgNP ↑, $AgNO_3$ ↑
30	Putative ferredoxin-NADP reductase, partial	Photosynthesis	AgNP ↓, $AgNO_3$ =
31, 32	33 kDa protein of oxygen evolving complex of photosystem II (Psb O)	Photosynthesis	AgNP ↑, $AgNO_3$ ↑
38, 39, 40, 41	Beta-carbonic anhydrase	Carbon utilization	AgNP ↑, $AgNO_3$ ↑
42	Triose phosphate isomerase cytosolic isoform-like	Glycolytic process	AgNP ↑, $AgNO_3$ ↑
43	Predicted protein XP_002330128.1	Calvin cycle	AgNP ↑, $AgNO_3$ ↑
48, 49, 50, 51, 52	23 kDa polypeptide of oxygen evolving complex of photosystem II, partial (PsbP)	Photosynthesis	AgNP ↑, $AgNO_3$ ↑
56	Ribulose-1,5-bisphosphate carboxylase/oxygenase large subunit, partial	Calvin cycle, photorespiration	AgNP =, $AgNO_3$ ↑
57, 58	PSI-D1 precursor (PsaD)	Photosynthesis	AgNP ↑, $AgNO_3$ ↑
59	PSI-E1 = 14.4 kda photosystem I psaE product (PsaE)	Photosynthesis	AgNP =, $AgNO_3$ ↓
60	17 kDa polypeptide of oxygen evolving complex of photosystem II (PsbQ)	Photosynthesis	AgNP ↑, $AgNO_3$ ↑
61	17 kDa polypeptide of oxygen evolving complex of photosystem II (PsbQ)	Photosynthesis	AgNP ↓, $AgNO_3$ =
62, 63	ATP synthase CF1 epsilon subunit	ATP synthesis coupled proton transport	AgNP ↑, $AgNO_3$ ↑
68	Putative ribulose bisphosphate carboxylase small subunit protein precursor	Photosynthesis	AgNP ↑, $AgNO_3$ ↑
Protein synthesis and processing			
2	Calreticulin	Protein folding	AgNP =, $AgNO_3$ ↑
11	Peptidyl-prolyl *cis-trans* isomerase, putative	Protein folding	AgNP ↑, $AgNO_3$ ↑
47	Nascent polypeptide associated complex alpha chain, partial	Protein transport	AgNP ↑, $AgNO_3$ ↑
53, 55	Cyclophilin	Protein folding	AgNP ↑, $AgNO_3$ ↑
64	Eukaryotic elongation factor 5A-1 isoform	Translation	AgNP =, $AgNO_3$ ↑

(*continued on next page*)

Table 3 (*continued*)

Spot(s) No.[a]	Protein name	Biological process[b]	Differential expression[c]
Defense and stress response			
1	Heat shock 70 protein	Protein folding, stress response	AgNP ↑, $AgNO_3$ ↑
4	*Predicted:* Protein disulphide-isomerase-like	Cellular redox homeostasis	AgNP =, $AgNO_3$ ↑
5	Chaperonin 60 alpha subunit, partial	Protein folding, stress response	AgNP =, $AgNO_3$ ↑
6	Beta chaperonin 60	Protein folding, stress response	AgNP ↓, $AgNO_3$ ↑
10	Ankyrin-repeat protein HBP1	Signal transduction, response to salt stress	AgNP ↑, $AgNO_3$ ↑
16	Salicylic acid binding catalase, partial	Response to oxidative stress	AgNP ↑, $AgNO_3$ ↑
17	Catalase 1	Response to oxidative stress	AgNP ↑, $AgNO_3$ ↑
26	Quinone oxidoreductase-like protein	Response to oxidative stress	AgNP ↑, $AgNO_3$ ↑
33, 34, 35	Ascorbate peroxidase	Response to oxidative stress	AgNP ↑, $AgNO_3$ ↑
37	Basic beta-1,3-glucanase	Hydrolase activity	AgNP ↑, $AgNO_3$ ↑
44	Iron superoxide dismutase (SOD)	Response to oxidative stress	AgNP ↑, $AgNO_3$ ↑
45	Chaperonin 21 precursor	Protein folding, positive regulation of SOD	AgNP ↑, $AgNO_3$ ↑
46	Acidic chitinase PR-P	Chitin degradation, plant defence	AgNP ↑, $AgNO_3$ ↑
54	*Predicted*: CBS domain-containing protein CBSX3, mitochondrial	Response to oxidative stress	AgNP =, $AgNO_3$ ↑
RNA processing			
23	mRNA-binding protein precursor, partial	RNA binding	AgNP ↑, $AgNO_3$ ↑
66	Glycine-rich RNA-binding protein	RNA binding and alternative mRNA splicing	AgNP ↑, $AgNO_3$ ↑
67	RNA-binding glycine rich protein 1a	RNA binding and alternative mRNA splicing	AgNP ↑, $AgNO_3$ ↑
Amino acid metabolism			
14, 15	Glutamine synthetase GS58 AAR86719.1	Glutamine biosynthetic process	AgNP ↑, $AgNO_3$ ↑
18	Aminomethyl-transferase, mitochondrial,	Glycine catabolic process	AgNP ↑, $AgNO_3$ ↑
19	Predicted: Aminomethyl-transferase, mitochondrial	Glycine catabolic process	AgNP ↑, $AgNO_3$ ↑
Nucleotide metabolism			
69	Nucleoside diphosphate kinase1	Synthesis of nucleoside triphosphates (other than ATP)	AgNP ↑, $AgNO_3$ ↑
Cell signal cascades			
65	Calmodulin-2 XP_002879035	Protein activity regulation by binding Ca^{2+} ions	AgNP =, $AgNO_3$ ↑
Unknown			
3, 36	Uncharacterized protein At5g39570-like		AgNP ↑, $AgNO_3$ ↑

[a] Spot number corresponds to the 2-DE gels presented in Supplement 1.
[b] Biological process was derived through Uniprot hit accessions for all identified proteins.
[c] Differential expression of protein spots if the spot volume is at least 1.5 × higher (↑) or 1.5 × lower (↓) compared to the control or of equal volume (=).

chloroplasts with dilated thylakoid systems. Jiang et al. (2014) also reported ultrastructural changes in chloroplasts of *Spirodela polyrhiza* exposed to AgNPs. In our previous study (Cvjetko et al., 2018), we found similar alterations in chloroplast ultrastructure in adult tobacco plants exposed to AgNPs as well as a strong decrease in PPX activity, which is in good correlation with the results obtained in

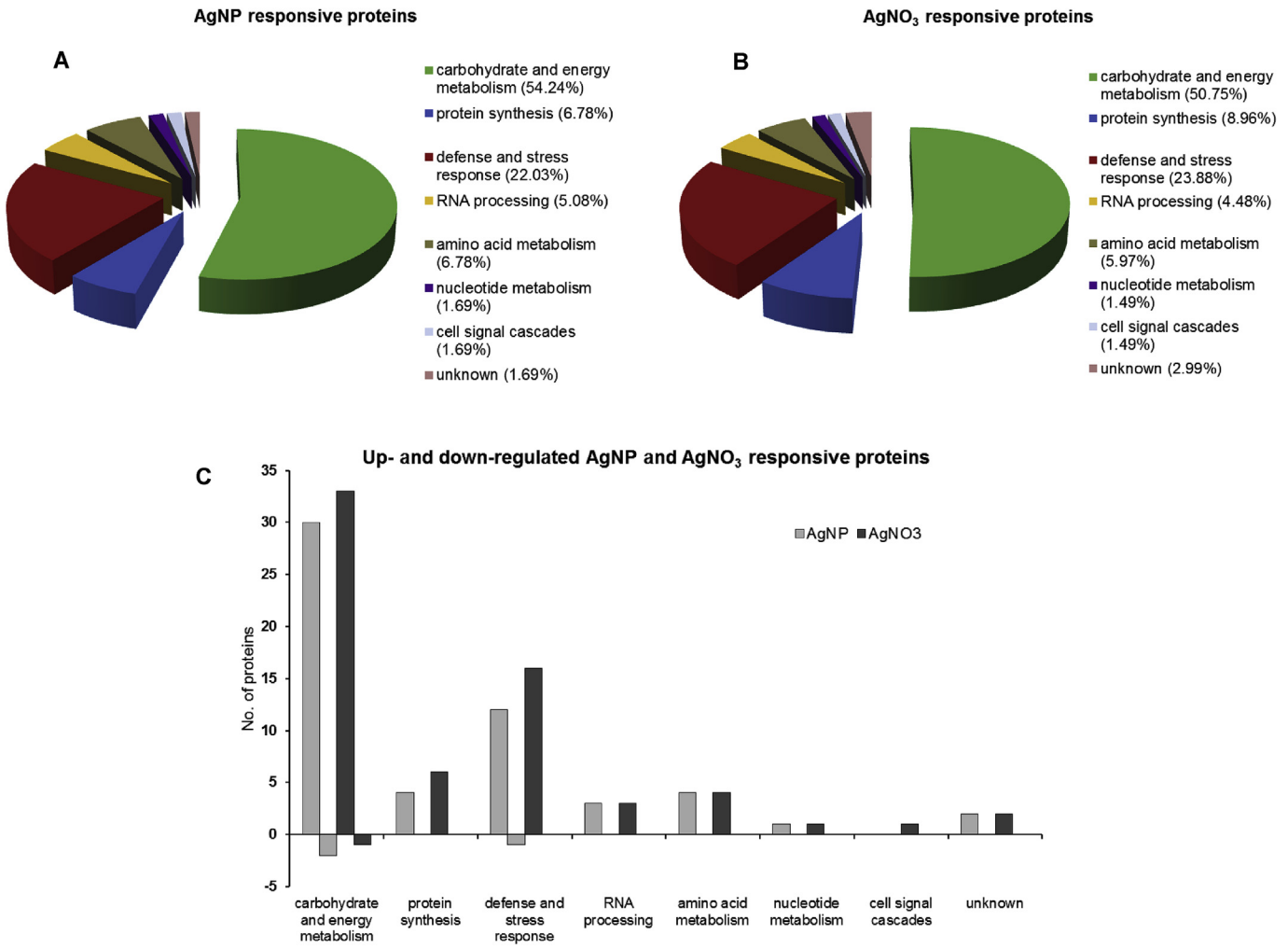

Fig. 4. Functional categorization of the differentially expressed proteins of tobacco seedlings treated with (A) 100 μM AgNPs and (B) 100 μM $AgNO_3$. Differentially expressed proteins identified by MALDI-TOF/TOF MS/MS were classified according to their putative biological process reported in the Uniprot database. (C) Analysis of responsiveness of differentially expressed proteins of tobacco seedlings exposed to either AgNPs or $AgNO_3$.

the seedlings and implies that AgNPs can contribute to the imbalance of chloroplast antioxidant system. To confirm whether these changes may be attributed to AgNPs, we have validated the stability of 100 μM AgNPs in the solid medium used for plant growth. UV–visible spectrophotometry measurement of 100 μM AgNPs solution in Milli-Q water revealed an absorption maximum at 424 nm, corresponding to surface plasmon resonance of AgNPs of approximately 50 nm, which is in correlation with manufacturer's report. Initial reduction of the absorption maximum immediately upon addition of AgNPs to the medium can be attributed to agglomeration of AgNPs (Gunsolus et al., 2015), while a maximum shift towards lower wavelengths may be ascribed to AgNPs oxidation and their dissolution in the medium (Zhu et al., 2012). However, over a period of three weeks the absorption maximum and its position have not changed significantly, which could be a result of AgNPs stabilization with Phytagel agar, natural polymer used for solidification of medium. It was reported that some polymer ligands can control access of molecular oxygen to the nanoparticle surface, which would decrease the oxidative dissolution rate of AgNPs (Gunsolus et al., 2015). Therefore, in our treatments with AgNPs, silver is available to seeds and developing seedlings in the form of nanoparticles, at least partially. Namely, the existence of ionic silver due to release from the surface of the particles cannot be completely excluded and may be responsible for toxic effects. Moreover, the exact fate of AgNPs in plant cells is very difficult to predict. It is known that in biological environments AgNPs interact readily with proteins and other biomolecules, which can alter the physico-chemical characteristics of AgNPs (Shannahan et al., 2013; Wen et al., 2013) and may also be responsible for the biological effects induced by nanoparticles. The biomolecules which associate with the AgNPs are dependent on the biological media and the physicochemical characteristics of nanomaterial (Nel et al., 2009; Walkey and Chan, 2012) and can enhance the AgNPs' resistance to transformation (Levak et al., 2017), or enhance their dissolution (Sharma et al., 2014). Thus, the system of nanoparticles in biota is not static but dynamic and many different processes are at play (Lundqvist et al., 2011; Wen et al., 2013).

Proteomic analysis showed that the majority of the identified proteins with differential expression after treatments with 100 μM AgNPs and $AgNO_3$ were those involved in the processes of primary metabolism ("carbohydrate and energy metabolism"), among which photosynthesis was found to the most impacted by the exposure of tobacco seedlings to AgNPs and $AgNO_3$. Four major protein complexes, photosystem (PS) I, PSII, the ATP synthase complex, and cytochrome *b*6/f complex are involved in the photosynthesis light-dependent reactions. In the PSI complex,

protein PsaE, crucial for ferredoxin (Fd) binding to PSI (Sétif et al., 2010), exhibited decreased expression during treatment with $AgNO_3$. In contrast, protein PsaD, which forms complexes with Fd and ferredoxin $NADP^+$ oxidoreductase (FNR) in PSI, was found to be up-regulated after both types of treatment. Moreover, FNR, responsible for the final step of linear electron flow transferring electrons from Fd to $NADP^+$, was also found to be up-regulated after exposure to $AgNO_3$. It is possible that the decreased electron transport caused by the down-regulation of PsaE induced the synthesis of PsaD and FNR to accelerate electron transfer and subsequently production of NADPH, which is required in the Calvin cycle. Similar behaviour of these proteins has already been reported as plant response to various abiotic stressors (Zörb et al., 2009; Pineda et al., 2010; Xu et al., 2015). Higher plants and green algae have a set of three extrinsic proteins in the oxygen-evolving complex of PSII: PsbO (33 kDa), PsbP (23 kDa) and PsbQ (17 kDa) (Ifuku and Noguchi, 2016). These proteins play important roles in maintaining optimal manganese, calcium and chloride concentrations at the active site of PSII (Bricker and Frankel, 2011). Recent studies have revealed their up-regulation after exposure of plants to various abiotic stresses (Gururani et al., 2013; Kang et al., 2017; Tamburino et al., 2017). In our study, these proteins were mostly up-regulated after exposure to either AgNPs or $AgNO_3$. ATP synthase CF1 epsilon subunit (plastid) also exhibited enhanced expression in our study after both types of treatments. ATP synthase CF1 generally takes part in ATP biosynthetic processes. Moreover, Vannini et al. (2013) reported that exposure of *Eruca sativa* to $AgNO_3$ caused up-regulation of several proteins important for energy production, including plastidial ATP synthase subunits. Ribulose-1,5-bisphospahte carboxylase/oxygenase (Rubisco), the key enzyme in photosynthesis carbon reactions, catalyses the conversion of atmospheric CO_2 into organic compounds. In our study, Rubisco small subunits were up-regulated after both types of treatments, as was Rubisco activase 2, the enzyme that is required for the activation of Rubisco, but may also have a role in stress acclimation (Chen et al., 2015). The expression of beta-carbonic anhydrase, which catalyses reversible conversion of HCO_3^- to CO_2, to ensure a sufficient amount of CO_2 for fixation by Rubisco, was also enhanced after exposure to both AgNPs and $AgNO_3$. Vannini et al. (2013) recorded carbonic anhydrase up-regulation in *E. sativa* plants exposed to $AgNO_3$, which corroborates our results. These findings suggest that the up-regulation of enzymes involved in photosynthesis might help seedlings exposed to AgNPs and $AgNO_3$ to accelerate their energy production and produce additional reducing power necessary to overcome (nano)silver-induced stress.

The enhanced expression of proteins involved in glycolysis i.e. plastidic aldolase, triose phosphate isomerase (TPI), glyceraldehyde-3-phosphate dehydrogenase (GAPDH) and 2,3-bisphosphoglycerate-independent phosphoglycerate mutase (iPGAM) was also recorded after exposure to either AgNPs or $AgNO_3$. These proteins improve a plant's ability to maintain glycolysis in order to ensure sufficient energy production. Moreover, TPI and GAPDH are multifunctional proteins, which display important functional diversity in mammals and plants (Zhang et al., 2011; Rogić et al., 2015). These "moonlighting" proteins exhibit activities distinct from their classical functions, such as involvement in oxidative stress response (Sirover, 2011). Namely, the up-regulation of TPI and GAPDH was observed under salinity and osmotic stress in several plant species (Caruso et al., 2008; Zhang et al., 2011; Rogić et al., 2015). As with photosynthesis, the enhanced expression of glycolytic proteins may serve to ensure sufficient energy to cope with oxidative stress in AgNP– and $AgNO_3$-exposed seedlings.

Among the proteins in the category "protein synthesis and processing", eukaryotic initiation factor 5A (eIF5A) was up-regulated after exposure to $AgNO_3$. This protein, apart from its role in protein synthesis regulation, translation elongation and mRNA turnover, was also found to be induced by abiotic stress. It can improve salt and heavy metal tolerance by increasing protein synthesis, enhancing ROS scavenging and the activities of antioxidant enzymes, as well as by preventing chlorophyll degradation and membrane damage (Wang et al., 2012). Moreover, Vannini et al. (2013) reported the up-regulation of eIF5A in *E. sativa* after exposure to $AgNO_3$, which corroborates our results. Among proteins involved in protein folding, cyclophilin and other peptidyl-prolyl *cis-trans* isomerases (PPIases) were up-regulated in seedlings exposed to AgNPs and $AgNO_3$, while calreticulin (Crt) exhibited enhanced expression only with $AgNO_3$. PPIases catalyse *cis-trans* isomerisation of the peptidyl-prolyl bond, which is a rate-limiting step in protein folding (Kaur et al., 2015). In Arabidopsis, the cytosolic PPIases were found to participate in plant-pathogen interaction and hormone signaling (Trupkin et al., 2012), while the chloroplast-localized isoform links light and redox signals to biosynthesis of cysteine and stress response (Dominguez-Solis et al., 2008). On the other hand, Crt is a unique Ca^{2+} binding chaperone of endoplasmic reticulum implicated in many cellular functions (Garg et al., 2015), including response to different environmental stimuli (Jia et al., 2009; Kim et al., 2013). Since it is known that Ag^+ acts on protein structure, enhanced abundance of proteins involved in protein synthesis and folding may have an important role in adaptation of plants to silver-imposed stress. The differential expression obtained after treatments with AgNPs and $AgNO_3$ confirms that $AgNO_3$ is more toxic to tobacco seedlings.

In the category "defense and stress response", several heat-shock proteins (Hsps) were identified. These proteins are responsible for the folding, assembly, translocation and degradation of proteins in many cellular processes (Wang et al., 2004). However, enhanced expression of Hsps has an important role in plants in response to a wide range of environmental stressors (Al-Whaibi, 2011); chloroplastic-like 20 kDa chaperonin protects photosynthesis during the heavy metal stress (Heckathorn et al., 2004), chloroplastic Hsp70 proteins have an important role in heavy metal response mechanisms involving the protection of cell membrane (Hall, 2002) while Hsp60 proteins are important in assisting plastid proteins such as Rubisco (Wang et al., 2004). Similarly, pathogenesis related (PR) proteins (β-1,3-glucanase and chitinase), usually induced in response to wounding or infection (Wu et al., 2001), are also involved in metal stress response (Beáta and Ildikó, 2011; Vannini et al., 2014). In our study, we found up-regulation of chloroplastic-like 20 kDa chaperonin, Hsp70 protein as well as PR proteins after exposure of tobacco seedlings to both AgNPs and $AgNO_3$, while two chloroplastic Hsp60 proteins exhibited enhanced expression after exposure to $AgNO_3$. Therefore, enhanced synthesis of Hsps and PR proteins as well as enhanced expression of several proteins involved in defence against oxidative stress (CAT, APX and Fe-SOD) in seedlings exposed to AgNPs and $AgNO_3$ could be one of the protective strategies against silver-induced toxicity.

Among proteins involved in the "RNA processing" category, two proteins were found to be up-regulated after both types of treatments; glycine-rich RNA binding protein (GRP) and mRNA-binding protein precursor. RNA-binding proteins are regulatory factors controlling posttranscriptional RNA metabolism during plant growth, development, and stress responses (Lorković, 2009; Xu et al., 2014; Lee and Kang, 2016). Moreover, it has been reported that some of the GRP family members have an impact on stress tolerance under different stress factors (Kim et al., 2007, 2008; Lee et al., 2009). Proteins identified as glutamine synthetases,

belonging to "amino acid metabolism" category, were also up-regulated in seedlings exposed to AgNPs and $AgNO_3$, indicating the importance of the carbon-nitrogen balance during adaptation to silver-induced stress, for glutamine synthetase is a key enzyme involved in ammonium metabolism, but it is also correlated with increased salt tolerance and photorespiration capacity (Hoshida et al., 2000). The up-regulation of calmodulin (CaM), one of the most extensively studied Ca^{2+}-sensing proteins involved in cell signaling, was also recorded in our study after $AgNO_3$-treatment. Intracellular changes in Ca^{2+} ions in response to different stimuli detected by calmodulin influence the activities of CaM-binding proteins, which have been implicated in plant adaptation to adverse environmental conditions (Wilkins et al., 2016).

Although some identified proteins exhibited different expression depending on type of exposure (AgNPs or $AgNO_3$), the majority of them were up-regulated by both treatments, thus indicating that dissociated silver could be involved in AgNP toxicity. Given the prolonged exposure of the seedlings to silver treatments (from seeds to fully developed seedlings), observed changes in the proteome are probably not the result of instant up-/down-regulation in response to (nano)silver, but rather reflect the adjustment of tobacco metabolism to nano(silver)-induced stress.

5. Conclusion

Despite the higher accumulation of Ag, treatments with nanosilver induced less severe oxidative damage in tobacco seedlings than silver applied in ionic form. The presence of nanoparticles was detected in root but not in leaf cells, although ultrastructural changes in chloroplast were found. Proteomic analysis revealed that most of the differentially expressed proteins in seedlings exposed to AgNPs and $AgNO_3$ overlapped and were up-regulated. However, the higher number of proteins induced by $AgNO_3$ confirms the lower toxicity of silver nanoparticles. The majority of the proteins up-regulated after the two types of treatments were those involved in the processes of primary metabolism, among which it was photosynthesis that was found to be the most significantly affected. It can be assumed that the enhanced energy production used to reinforce defensive mechanisms enables plants to cope with silver-induced toxicity.

Acknowledgments

Oxidative stress analyses were supported by the Croatian Science Foundation [grant number IP-2014-09-6488]. The financial support for proteomic analyses was provided by the European Social Fund [grant number HR.3.2.01–0095] and the University of Zagreb [grant number 20281222]. TEM analyses have received funding from the European Union Seventh Framework Programme under Grant Agreement 312483 - ESTEEM2 (Integrated Infrastructure Initiative–I3). Tobacco seeds were provided from the Zagreb Tobacco Institute.

Appendix A. Supplementary data

Supplementary data related to this article can be found at https://doi.org/10.1016/j.chemosphere.2018.06.128.

References

Abdal Dayem, A., Hossain, M., Lee, S., Kim, K., Saha, S., Yang, G.M., Choi, H., Cho, S.G., 2017. The role of reactive oxygen species (ROS) in the biological activities of metallic nanoparticles. Int. J. Mol. Sci. 18, 120. https://doi.org/10.3390/ijms18010120.

Aebi, H., 1984. Catalase in vitro. Methods Enzymol. 105, 121–126. https://doi.org/10.1016/S0076-6879(84)05016-3.

Ahamed, M., Posgai, R., Gorey, T.J., Nielsen, M., Hussain, S.M., Rowe, J.J., 2010. Silver nanoparticles induced heat shock protein 70, oxidative stress and apoptosis in *Drosophila melanogaster*. Toxicol. Appl. Pharmacol. 242, 263–269. https://doi.org/10.1016/j.taap.2009.10.016.

Al-Whaibi, M.H., 2011. Plant heat-shock proteins: a mini review. J. King Saud Univ. Sci. 23, 139–150. https://doi.org/10.1016/j.jksus.2010.06.022.

Beáta, P., Ildikó, M., 2011. Plant defense against heavy metals: the involvement of pathogenesis-related (PR) proteins. Recent Progress in Medicinal Plants. In: Awaad, A.S., Kaushik, G., Govil, J.N. (Eds.), Mechanism and action of phyto-constituents, vol. 31. Studium Press (India) Pvt. Ltd, New Delhi, pp. 179–205.

Beauchamp, C., Fridovich, I., 1971. Superoxide dismutase: improved assays and an assay applicable to acrylamide gels. Anal. Biochem. 44, 276–287. https://doi.org/10.1016/0003-2697(71)90370-8.

Beer, C., Foldbjerg, R., Hayashi, Y., Sutherland, D.S., Autrup, H., 2012. Toxicity of silver nanoparticles - nanoparticle or silver ion? Toxicol. Lett. 208, 286–292. https://doi.org/10.1016/j.toxlet.2011.11.002.

Bradford, M.M., 1976. A rapid and sensitive method for the quantification of microgram quantities of protein utilizing the principle of protein – dye binding. Anal. Biochem. 72, 248–254. https://doi.org/10.1016/0003-2697(76)90527-3.

Bricker, T.M., Frankel, L.K., 2011. Auxiliary functions of the PsbO, PsbP and PsbQ proteins of higher plant Photosystem II: a critical analysis. J. Photochem. Photobiol., B 104 (1–2), 165–178. https://doi.org/10.1016/j.jphotobiol.2011.01.025.

Calderón-Jiménez, B., Johnson, M.E., Montoro Bustos, A.R., Murphy, K.E., Winchester, M.R., Vega Baudrit, J.R., 2017. Silver nanoparticles: technological advances, societal impacts, and metrological challenges. Front. Chem. 5, 6. https://doi.org/10.3389/fchem.2017.00006.

Caruso, G., Cavaliere, C., Guarino, C., Gubbiotti, R., Foglia, P., Laganà, A., 2008. Identification of changes in *Triticum durum* L. leaf proteome in response to salt stress by two-dimensional electrophoresis and MALDI-TOF mass spectrometry. Anal. Bioanal. Chem. 391, 381–390. https://doi.org/10.1007/s00216-008-2008-x.

Castiglioni, S., Caspani, C., Cazzaniga, A., Maier, J.A., 2014. Short- and long-term effects of silver nanoparticles on human microvascular endothelial cells. World J. Biol. Chem. 5, 457–464. https://doi.org/10.4331/wjbc.v5.i4.457.

Chen, Y., Wang, X.M., Zhou, L., He, Y., Wang, D., Qi, Y.H., Jiang, D.A., 2015. Rubisco activase is also a multiple responder to abiotic stresses in rice. PLoS One 10 (10), e0140934. https://doi.org/10.1371/journal.pone.0140934.

Cvjetko, P., Zovko, M., Balen, B., 2014. Proteomics of heavy metal toxicity in plants. Arh. Hig. Rada. Toksikol. https://doi.org/10.2478/10004-1254-65-2014-2443.

Cvjetko, P., Milošić, A., Domijan, A.M., Vinković Vrček, I., Tolić, S., Peharec Štefanić, P., Letofsky-Papst, I., Tkalec, M., Balen, B., 2017. Toxicity of silver ions and differently coated silver nanoparticles in *Allium cepa* roots. Ecotoxicol. Environ. Saf. 137, 18–28. https://doi.org/10.1016/j.ecoenv.2016.11.009.

Cvjetko, P., Zovko, M., Peharec Štefanić, P., Biba, R., Tkalec, M., Domijan, A.M., Vinković Vrček, I., Letofsky-Papst, I., Šikić, S., Balen, B., 2018. Phytotoxic effects of silver nanoparticles in tobacco plants. Environ. Sci. Pollut. Res. Int. 25 (6), 5590–5602. https://doi.org/10.1007/s11356-017-0928-8.

Dominguez-Solis, J.R., He, Z., Lima, A., Ting, J., Buchanan, B.B., Luan, S., 2008. A cyclophilin links redox and light signals to cysteine biosynthesis and stress responses in chloroplasts. Proc. Natl. Acad. Sci. U.S.A. 105, 16386–16391. https://doi.org/10.1073/pnas.0808204105\r0808204105.

El-Temsah, Y.S., Joner, E.J., 2012. Impact of Fe and Ag nanoparticles on seed germination and differences in bioavailability during exposure in aqueous suspension and soil. Environ. Toxicol. 27, 42–49. https://doi.org/10.1002/tox.20610.

Faurobert, M., Pelpoir, E., Chaib, J., 2007. Phenol extraction of proteins for proteomic studies of recalcitrant plant tissues. Meth. Mol. Biol. 355, 9–14. https://doi.org/10.1385/1-59745-227-0:9.

Ganapathi, T.R., Suprasanna, P., Rao, P.S., Bapat, V.A., 2004. Tobacco (*Nicotiana tabacum* L.) - a model system for tissue culture interventions and genetic engineering. Indian J. Biotechnol. 3 (2), 171–184.

Garg, G., Yadav, S., Ruchi Yadav, G., 2015. Key roles of calreticulin and calnexin proteins in plant perception under stress conditions: a review. Adv. Life Sci. 5, 18–26.

Ghandour, W., Hubbard, J.A., Deistung, J., Hughes, M.N., Poole, R.K., 1988. The uptake of silver ions by *Escherichia coli* K12: toxic effects and interaction with copper ions. Appl. Microbiol. Biotechnol. 28, 559–565. https://doi.org/10.1007/BF00250412.

Gichner, T., Patková, Z., Száková, J., Demnerová, K., 2004. Cadmium induces DNA damage in tobacco roots, but no DNA damage, somatic mutations or homologous recombination in tobacco leaves. Mutat. Res. 559, 49–57. https://doi.org/10.1016/j.mrgentox.2003.12.008.

Gunsolus, I.L., Mousavi, M.P., Hussein, K., Bühlmann, P.1, Haynes, C.L., 2015. Effects of humic and fulvic acids on silver nanoparticle stability, dissolution, and toxicity. Environ. Sci. Technol. 49 (13), 8078–8806. https://doi.org/10.1021/acs.est.5b01496.

Gururani, M.A., Upadhyaya, C.P., Strasser, R.J., Yu, J.W., Park, S.W., 2013. Evaluation of abiotic stress tolerance in transgenic potato plants with reduced expression of PSII manganese stabilizing protein. Plant Sci. 198, 7–16. https://doi.org/10.1016/j.plantsci.2012.09.014.

Gygi, S.P., Aebersold, R., 2000. Mass spectrometry and proteomics. Curr. Opin. Chem. Biol. 4, 489–494. https://doi.org/10.1016/S1367-5931(00)00121-6.

Hall, J.L., 2002. Cellular mechanisms for heavy metal detoxification and tolerance. J. Exp. Bot. 53, 1–11. https://doi.org/10.1093/jxb/53.366.1.

Hatami, M., Ghorbanpour, M., 2013. Effect of nanosilver on physiological

performance of Pelargonium plants exposed to dark storage. J. Hortic. Res. 21, 15–20. https://doi.org/10.2478/johr-2013-0003.
Heath, R.L., Packer, L., 1968. Photoperoxidation in isolated chloroplasts. I. Kinetics and stoichiometry of fatty acid peroxidation. Arch. Biochem. Biophys. 125, 189–198. https://doi.org/10.1016/0003-9861(68)90654-1.
Heckathorn, S.A., Mueller, J.K., Laguidice, S., Zhu, B., Barrett, T., Blair, B., Dong, Y., 2004. Chloroplast small heat-shock proteins protect photosynthesis during heavy metal stress. Am. J. Bot. 91, 1312–1318. https://doi.org/10.3732/ajb.91.9.1312.
Hoshida, H., Tanaka, Y., Hibino, T., Hayashi, Y., Tanaka, A., Takabe, T., Takabe, T., 2000. Enhanced tolerance to salt stress in transgenic rice that overexpresses chloroplast glutamine synthetase. Plant Mol. Biol. 43, 103–111. https://doi.org/10.1023/A:1006408712416.
Hossain, Z., Komatsu, S., 2013. Contribution of proteomic studies towards understanding plant heavy metal stress response. Front. Plant Sci. 3, 310. https://doi.org/10.3389/fpls.2012.00310.
Ifuku, K., Noguchi, T., 2016. Structural coupling of extrinsic proteins with the oxygen-evolving center in photosystem II. Front. Plant Sci. 7, 84. https://doi.org/10.3389/fpls.2016.00084.
Jia, X.Y., He, L.H., Jing, R.L., Li, R.Z., 2009. Calreticulin: conserved protein and diverse functions in plants. Physiol. Plant 136, 127–138. https://doi.org/10.1111/j.1399-3054.2009.01223.x.
Jiang, H.S., Qiu, X.N., Li, G.B., Li, W., Yin, L.Y., 2014. Silver nanoparticles induced accumulation of reactive oxygen species and alteration of antioxidant systems in the aquatic plant *Spirodela polyrhiza*. Environ. Toxicol. Chem. 33, 1398–1405. https://doi.org/10.1002/etc.2577.
Kang, L., Kim, H.S., Kwon, Y.S., Ke, Q., Ji, C.Y., Park, S.C., Lee, H.-S., Deng, X., Kwak, S.S., 2017. IbOr regulates photosynthesis under heat stress by stabilizing IbPsbP in sweetpotato. Front. Plant Sci. 8, 989. https://doi.org/10.3389/fpls.2017.00989.
Kaur, G., Singh, S., Singh, H., Chawla, M., Dutta, T., Kaur, H., Bender, K., Snedden, W.A., Kapoor, S., Pareek, A., Singh, P., 2015. Characterization of peptidyl-prolyl *cis-trans* isomerase- and calmodulin-binding activity of a cytosolic *Arabidopsis thaliana* Cyclophilin AtCyp19-3. PLoS One 10 (8), e0136692. https://doi.org/10.1371/journal.pone.0136692.
Kim, J.H., Nguyen, N.H., Nguyen, N.T., Hong, S.W., Lee, H., 2013. Loss of all three calreticulins, CRT1, CRT2 and CRT3, causes enhanced sensitivity to water stress in Arabidopsis. Plant Cell Rep. 32, 1843–1853. https://doi.org/10.1007/s00299-013-1497-z.
Kim, J.S., Jung, H.J., Lee, H.J., Kim, K.A., Goh, C.H., Woo, Y., Oh, S.H., Han, Y.S., Kang, H., 2008. Glycine-rich RNA-binding protein 7 affects abiotic stress responses by regulating stomata opening and closing in *Arabidopsis thaliana*. Plant J. 55, 455–466. https://doi.org/10.1111/j.1365-313X.2008.03518.x.
Kim, J.Y., Park, S.J., Jang, B., Jung, C.-H., Ahn, S.J., Goh, C.-H., Cho, K., Han, O., Kang, H., 2007. Functional characterization of a glycine-rich RNA-binding protein 2 in *Arabidopsis thaliana* under abiotic stress conditions. Plant J. 50, 439–451. https://doi.org/10.1111/j.1365-313X.2007.03057.x.
Kim, S., Choi, J.E., Choi, J., Chung, K.H., Park, K., Yi, J., Ryu, D.Y., 2009. Oxidative stress-dependent toxicity of silver nanoparticles in human hepatoma cells. Toxicol. Vitro 23, 1076–1084. https://doi.org/10.1016/j.tiv.2009.06.001.
Lee, K., Kang, H., 2016. Emerging roles of RNA-binding proteins in plant growth, development, and stress responses. Mol. Cells 39, 179–185. https://doi.org/10.14348/molcells.2016.2359.
Lee, M.O., Kim, K.P., Kim, B.G., Hahn, J.S., Hong, C.B., 2009. Flooding stress-induced glycine-rich RNA-binding protein from *Nicotiana tabacum*. Mol. Cells 27, 47–54. https://doi.org/10.1007/s10059-009-0004-4.
Lee, W.M., Kwak II, J., An, Y.J., 2012. Effect of silver nanoparticles in crop plants *Phaseolus radiatus* and *Sorghum bicolor*: media effect on phytotoxicity. Chemosphere 86, 491–499. https://doi.org/10.1016/j.chemosphere.2011.10.013.
Levak, M., Burić, P., Dutour Sikirić, M., Domazet Jurašin, D., Mikac, N., Bačić, N., Drexel, R., Meier, F., Jakšić, Ž., Lyons, D.M., 2017. Effect of protein corona on silver nanoparticle stabilization and ion release kinetics in artificial seawater. Environ. Sci. Technol. 51 (3), 1259–1266. https://doi.org/10.1021/acs.est.6b03161.
Levine, R.L., Garland, D., Oliver, C.N., Amici, A., Climent, I., Lenz, A.G., Ahn, B.W., Shaltiel, S., Stadtman, E.R., 1990. Determination of carbonyl content in oxidatively modified proteins. Methods Enzymol. 186, 464–478. https://doi.org/10.1016/0076-6879(90)86141-H.
Lichtenthaler, H.K., 1987. Chlorophylls and carotenoids: pigments of photosynthetic membranes. Methods Enzymol. 148, 350–382.
Lorković, Z.J., 2009. Role of plant RNA-binding proteins in development, stress response and genome organization. Trends Plant Sci. 14 (4), 229–236. https://doi.org/10.1016/j.tplants.2009.01.007.
Lundqvist, M., Stigler, J., Cedervall, T., Berggård, T., Flanagan, M.B., Lynch, I., Elia, G., Dawson, K., 2011. The evolution of the protein corona around nanoparticles: a test study. ACS Nano 5 (9), 7503–7509. https://doi.org/10.1021/nn202458g.
Majsec, K., Cvjetko, P., Tolić, S., Tkalec, M., Balen, B., Pavlica, M., 2016. Integrative approach gives new insights into combined Cd/Cu exposure in tobacco. Acta Physiol. Plant. 38, 142. https://doi.org/10.1007/s11738-016-2158-y.
Maynard, A.D., Warheit, D.B., Philbert, M.A., 2011. The new toxicology of sophisticated materials: nanotoxicology and beyond. Toxicol. Sci. https://doi.org/10.1093/toxsci/kfq372.
Mirzajani, F., Askari, H., Hamzelou, S., Farzaneh, M., Ghassempour, A., 2013. Effect of silver nanoparticles on *Oryza sativa* L. and its rhizosphere bacteria. Ecotoxicol. Environ. Saf. 88, 48–54. https://doi.org/10.1016/j.ecoenv.2012.10.018.
Murashige, T., Skoog, F., 1962. A revised medium for rapid growth and bioassay with tobacco tissue culture. Physiol. Plant 15, 473–497. https://doi.org/10.1111/j.1399-3054.1962.tb08052.x.
Mustafa, G., Sakata, K., Hossain, Z., Komatsu, S., 2015. Proteomic study on the effects of silver nanoparticles on soybean under flooding stress. J. Proteomics 122, 100–118. https://doi.org/10.1016/j.jprot.2015.03.030.
Mytych, J., Zebrowski, J., Lewinska, A., Wnuk, M., 2017. Prolonged effects of silver nanoparticles on p53/p21 pathway-mediated proliferation, DNA damage response, and methylation parameters in HT22 hippocampal neuronal cells. Mol. Neurobiol. 54, 1285–1300. https://doi.org/10.1007/s12035-016-9688-6L.
Nair, P.M.G., Chung, I.M., 2014a. Assessment of silver nanoparticle-induced physiological and molecular changes in *Arabidopsis thaliana*. Environ. Sci. Pollut. Res. 21, 8858–8869. https://doi.org/10.1007/s11356-014-2822-y.
Nair, P.M.G., Chung, I.M., 2014b. Physiological and molecular level effects of silver nanoparticles exposure in rice (*Oryza sativa* L.) seedlings. Chemosphere 112, 105–113. https://doi.org/10.1016/j.chemosphere.2014.03.056.
Nakano, Y., Asada, K., 1981. Hydrogen peroxide is scavenged by ascorbate-specific peroxidase in spinach chloroplasts. Plant Cell Physiol. 22, 867–880. https://doi.org/10.1093/oxfordjournals.pcp.a076232.
Navarro, E., Baun, A., Behra, R., Hartmann, N.B., Filser, J., Miao, A.J., Quigg, A., Santschi, P.H., Sigg, L., 2008a. Environmental behavior and ecotoxicity of engineered nanoparticles to algae, plants, and fungi. Ecotoxicology 17 (5), 372–386. https://doi.org/10.1007/s10646-008-0214-0.
Navarro, E., Piccapietra, F., Wagner, B., Marconi, F., Kaegi, R., Odzak, N., Sigg, L., Behra, R., 2008b. Toxicity of silver nanoparticles to *Chlamydomonas reinhardtii*. Environ. Sci. Technol. 42, 8959–8964. https://doi.org/10.1021/es801785m.
Nel, A.E., Mädler, L., Velegol, D., Xia, T., Hoek, E.M.V., Somasundaran, P., Klaessig, F., Castranova, V., Thompson, M., 2009. Understanding biophysicochemical interactions at the nano-bio interface. Nat. Mater. 8, 543–557.
Patlolla, A.K., Berry, A., May, L., Tchounwou, P.B., 2012. Genotoxicity of silver nanoparticles in *Vicia faba*: a pilot study on the environmental monitoring of nanoparticles. Int. J. Environ. Res. Publ. Health 9 (5), 1649–1662. https://doi.org/10.3390/ijerph9051649.
Pavoković, D., Križnik, B., Krsnik-Rasol, M., 2012. Evaluation of protein extraction methods for proteomic analysis of non-model recalcitrant plant tissues. Croat. Chem. Acta 85, 177–183. https://doi.org/10.5562/cca1804.
Peharec Štefanić, P., Šikić, S., Cvjetko, P., Balen, B., 2012. Cadmium and zinc induced similar changes in protein and glycoprotein patterns in tobacco (*Nicotiana tabacum* L.) seedlings and plants. Arh. Hig. Rada. Toksikol. 63, 321–335. https://doi.org/10.2478/10004-1254-63-2012-2173.
Piccapietra, F., Allué, C.G., Sigg, L., Behra, R., 2012. Intracellular silver accumulation in *Chlamydomonas reinhardtii* upon exposure to carbonate coated silver nanoparticles and silver nitrate. Environ. Sci. Technol. 46, 7390–7397. https://doi.org/10.1021/es300734m.
Pineda, M., Sajnani, C., Barón, M., 2010. Changes induced by the Pepper mild mottle tobamovirus on the chloroplast proteome of *Nicotiana benthamiana*. Photosynth. Res. 103, 31–45. https://doi.org/10.1007/s11120-009-9499-y.
Powers, C.M., Slotkin, T.A., Seidler, F.J., Badireddy, A.R., Padilla, S., 2011. Silver nanoparticles alter zebrafish development and larval behavior: distinct roles for particle size, coating and composition. Neurotoxicol. Teratol. 33, 708–714. https://doi.org/10.1016/j.ntt.2011.02.002.
Poynton, H.C., Lazorchak, J.M., Impellitteri, C.A., Blalock, B.J., Rogers, K., Allen, H.J., Loguinov, A., Heckman, J.L., Govindasmawy, S., 2012. Toxicogenomic responses of nanotoxicity in *Daphnia magna* exposed to silver nitrate and coated silver nanoparticles. Environ. Sci. Technol. 46, 6288–6296. https://doi.org/10.1021/es3001618.
Qian, H., Peng, X., Han, X., Ren, J., Sun, L., Fu, Z., 2013. Comparison of the toxicity of silver nanoparticles and silver ions on the growth of terrestrial plant model *Arabidopsis thaliana*. J. Environ. Sci. 25, 1947–1955. https://doi.org/10.1016/S1001-0742(12)60301-5.
Qin, Y., Zhang, S., Zhang, L., Zhu, D., Syed, A., 2005. Response of in vitro strawberry to silver nitrate ($AgNO_3$). Hortscience 40, 747–751.
Rani, P.U., Yasur, J., Loke, K.S., Dutta, D., 2016. Effect of synthetic and bio-synthesized silver nanoparticles on growth, physiology and oxidative stress of water hyacinth: *Eichhornia crassipes* (Mart) Solms. Acta Physiol. Plant. 38, 1–9.
Rogić, T., Horvatić, A., Tkalec, M., Cindrić, M., Balen, B., 2015. Proteomic analysis of *Mammillaria gracilis* Pfeiff. in vitro-grown cultures exposed to iso-osmotic NaCl and mannitol. Plant Cell Tiss. Organ. Cult. 122, 127–146. https://doi.org/10.1007/s11240-015-0756-9.
Saha, N., Dutta Gupta, S., 2017. A glimpse on silver nanoparticles genotoxicity in higher plants. Glob. J. Nanomed. 2 (2), 555583.
Schaeffer, S., Koepke, T., Dhingra, A., 2012. Tobacco: a Model Plant for Understanding the Mechanism of Abiotic Stress Tolerance. Improving Crop Resistance to Abiotic Stress. Chapter 46. Wiley-VCH Verlag GmbH & Co. KGaA.
Sétif, P., Harris, N., Lagoutte, B., Dotson, S., Weinberger, S.R., 2010. Detection of the photosystem I: ferredoxin complex by backscattering interferometry. J. Am. Chem. Soc. 132, 10620–10622. https://doi.org/10.1021/ja102208u.
Shannahan, J.H., Lai, X., Ke, P.C., Podila, R., Brown, J.M., Witzmann, F.A., 2013. Silver nanoparticle protein corona composition in cell culture media. PLoS One 8 (9), e74001. https://doi.org/10.1371/journal.pone.007400.
Sharma, S., Mustafiz, A., Singla-Pareek, S., Shankar Srivastava, P., Sopory, S., 2012. Characterization of stress and methylglyoxal inducible triose phosphate isomerase (OscTPI) from rice. Plant Signal. Beyond Behav. 7, 1337–1345. https://doi.org/10.4161/psb.21415.
Sharma, V.K., Siskova, K.M., Zboril, R., Gardea-Torresdey, J.L., 2014. Organic-coated silver nanoparticles in biological and environmental conditions: fate, stability and toxicity. Adv. Colloid Interface Sci. 204, 15–34. https://doi.org/10.1016/

j.cis.2013.12.002.
Shevchenko, A., Wilm, M., Vorm, O., Mann, M., 1996. Mass spectrometric sequencing of proteins from silver-stained polyacrylamide gels. Anal. Chem. 68, 850–858. https://doi.org/10.1021/ac950914h.
Sierro, N., Battey, J.N., Ouadi, S., Bakaher, N., Bovet, L., Willig, A., Goepfert, S., Peitsch, M.C., Ivanov, N.V., 2014. The tobacco genome sequence and its comparison with those of tomato and potato. Nat. Commun. 5, 3833. https://doi.org/10.1038/ncomms4833.
Sirover, M.A., 2011. On the functional diversity of glyceraldehyde-3-phosphate dehydrogenase: biochemical mechanisms and regulatory control. Biochim. Biophys. Acta 1810, 741–751. https://doi.org/10.1016/j.bbagen.2011.05.010.
Tamburino, R., Vitale, M., Ruggiero, A., Sassi, M., Sannino, L., Arena, S., Costa, A., Batelli, G., Zambrano, N., Scaloni, A., Grillo, S., Scotti, N., 2017. Chloroplast proteome response to drought stress and recovery in tomato (*Solanum lycopersicum* L.). BMC Plant Biol. 17, 40. https://doi.org/10.1186/s12870-017-0971-0.
Tkalec, M., Peharec Štefanić, P., Cvjetko, P., Šikić, S., Pavlica, M., Balen, B., 2014. The effects of cadmium-zinc interactions on biochemical responses in tobacco seedlings and adult plants. PLoS One 9 (1), e87582. https://doi.org/10.1371/journal.pone.0087582.
Tripathi, D.K., Tripathi, A., Shweta, Singh, S., Singh, Y., Vishwakarma, K., Yadav, G., Sharma, S., Singh, V.K., Mishra, R.K., Upadhyay, R.G., Dubey, N.K., Lee, Y., Chauhan, D.K., 2017. Uptake, accumulation and toxicity of silver nanoparticle in autotrophic plants, and heterotrophic microbes: a concentric review. Front. Microbiol. https://doi.org/10.3389/fmicb.2017.00007.
Trupkin, S.A., Mora-García, S., Casal, J.J., 2012. The cyclophilin ROC1 links phytochrome and cryptochrome to brassinosteroid sensitivity. Plant J. 71, 712–723. https://doi.org/10.1111/j.1365-313X.2012.05013.x.
Vannini, C., Domingo, G., Onelli, E., Prinsi, B., Marsoni, M., Espen, L., Bracale, M., 2013. Morphological and proteomic responses of *Eruca sativa* exposed to silver nanoparticles or silver nitrate. PLoS One 8 (7), e68752. https://doi.org/10.1371/journal.pone.0068752.
Vannini, C., Domingo, G., Onelli, E., De Mattia, F., Bruni, I., Marsoni, M., Bracale, M., 2014. Phytotoxic and genotoxic effects of silver nanoparticles exposure on germinating wheat seedlings. J. Plant Physiol. 171, 1142–1148. https://doi.org/10.1016/j.jplph.2014.05.002.
Walkey, C.D., Chan, W.C., 2012. Understanding and controlling the interaction of nanomaterials with proteins in a physiological environment. Chem. Soc. Rev. 41 (7), 2780–2799. https://doi.org/10.1039/c1cs15233e.
Wang, L., Xu, C., Wang, C., Wang, Y., 2012. Characterization of a eukaryotic translation initiation factor 5A homolog from *Tamarix androssowii* involved in plant abiotic stress tolerance. BMC Plant Biol. 12, 118. https://doi.org/10.1186/1471-2229-12-118.
Wang, W., Vinocur, B., Shoseyov, O., Altman, A., 2004. Role of plant heat-shock proteins and molecular chaperones in the abiotic stress response. Trends Plant Sci. https://doi.org/10.1016/j.tplants.2004.03.006.
Wellburn, A.R., 1994. The spectral determination of chlorophylls a and b, as well as total carotenoids, using various solvents with spectrophotometers of different resolution. J. Plant Physiol. 144, 307–313.
Wen, Y.M., Geitner, N.K., Chen, R., Ding, F., Chen, P.Y., Andorfer, R.E., Govindan, P.N., Ke, P.C., 2013. Binding of cytoskeletal proteins with silver nanoparticles. RSC Adv. 3, 22002–22007. https://doi.org/10.1039/c3ra43281e.
Wilkins, K.A., Matthus, E., Swarbreck, S.M., Davies, J.M., 2016. Calcium-mediated abiotic stress signaling in roots. Front. Plant Sci. 7, 1296. https://doi.org/10.3389/fpls.2016.01296.
Wu, C.T., Leubner-Metzger, G., Meins, F., Bradford, K.J., 2001. Class I beta-1,3-glucanase and chitinase are expressed in the micropylar endosperm of tomato seeds prior to radicle emergence. Plant Physiol. 126, 1299–1313. https://doi.org/10.1104/PP.126.3.1299.
Xu, J., Lan, H., Fang, H., Huang, X., Zhang, H., Huang, J., 2015. Quantitative proteomic analysis of the rice (*Oryza sativa* L.) salt response. PLoS One 10 (3), e0120978. https://doi.org/10.1371/journal.pone.0120978.
Xu, T., Gu, L., Choi, M.J., Kim, R.J., Suh, M.C., Kang, H., 2014. Comparative functional analysis of wheat (*Triticum aestivum*) zinc finger-containing glycine-rich RNA-binding proteins in response to abiotic stresses. PLoS One 9 (5), e96877. https://doi.org/10.1371/journal.pone.0096877.
Yin, L., Cheng, Y., Espinass, B., Colman, B.P., Auffan, M., Wiesner, M., Rose, J., Liu, J., Bernhardt, E.S., 2011. More than the ions: the effects of silver nanoparticles on *Lolium multiflorum*. Environ. Sci. Technol. 45 (6), 2360–2367. https://doi.org/10.1021/es103995x.
Yin, L., Colman, B.P., McGill, B.M., Wright, J.P., Bernhardt, E.S., 2012. Effects of silver nanoparticle exposure on germination and early growth of eleven wetland plants. PLoS One 7 (10), e47674. https://doi.org/10.1371/journal.pone.0047674.
Zhang, T., Wang, L., Chen, Q., Chen, C., 2014. Cytotoxic potential of silver nanoparticles. Yonsei Med. J. 55, 283–291. https://doi.org/10.3349/ymj.2014.55.2.283.
Zhang, X.-F., Liu, Z.-G., Shen, W., Gurunathan, S., 2016. Silver nanoparticles: synthesis, characterization, properties, applications, and therapeutic approaches. Int. J. Mol. Sci. 17 (9), 1534. https://doi.org/10.3390/ijms17091534.
Zhang, X.H., Rao, X.L., Shi, H.T., Li, R.J., Lu, Y.T., 2011. Overexpression of a cytosolic glyceraldehyde-3-phosphate dehydrogenase gene OsGAPC3 confers salt tolerance in rice. Plant Cell Tiss. Organ. Cult. 107, 1–11. https://doi.org/10.1007/s11240-011-9950-6.
Zhu, M., Nie, G., Meng, H., Xia, T., Nel, A., Zhao, Y., 2012. Physicochemical properties determine nanomaterial cellular uptake, transport and fate. Acc. Chem. Res. 46, 622–631. https://doi.org/10.1021/ar300031y.
Zörb, C., Herbst, R., Forreiter, C., Schubert, S., 2009. Short-term effects of salt exposure on the maize chloroplast protein pattern. Proteomics 9, 4209–4220. https://doi.org/10.1002/pmic.200800791.